Int. J. Nonlinear Anal. Appl. 14 (2023) 1, 805–818
ISSN: 2008-6822 (electronic)
http://dx.doi.org/10.22075/ijnaa.2022.22977.2444

Transient thermoelastic bending analysis of a rectangular plate with a simply supported edge under heat source: Green's function approach

Kishor R. Gaikwad[a,*], Yogesh U. Naner[b], Satish G. Khavale[a]

[a]Department of Mathematics, N. E. S., Science College, Nanded, Maharashtra, 431605, India

[b]Department of Mathematics, Shri Vitthal Rukhmini Art's, Commerce and Science College, Sawana, Yavatmal, Maharashtra, India

(Communicated by Saman Babaie-Kafaki)

Abstract

The aim of the current research is to analyze the transient thermoelastic bending analysis of a rectangular plate with a simply supported edge under the heat source. Initially, the plate is kept at a constant temperature. For $t > 0$, the heat is produced in the plate at the rate $g(W.m^{-3})$ and the surfaces at $x = 0, a$ and $y = 0, b$ are kept at zero temperature, while the surfaces $z = 0, c$ are subjected to heat convection. Using Green's function approach and integral transform technique, the analytical solution of the rectangular plate with the simply supported edge is derived. As a preeminent finding from this investigation, it can be deduced that the accuracy, reliability, and simplicity of these methods are excellent. Accurate bending solutions to title problems are then obtained using the transform technique. The approach used in this paper is more reasonable than conventional methods. Numerical results are presented to demonstrate the validity and efficiency of the approach as compared with those reported in other literature. The outcomes demonstrate that the temperature profile and the thermal deflection are maximum at the middle part of the plate, due to the heat source located in the middle, however, the direction of heat flow and the body deformation is the same.

Keywords: Green's Function, Rectangular plate, Heat Source, Thermal Bending, Thermal Stresses
2020 MSC: 35B07, 35G30, 35K05, 44A10

1 Introduction

The thin rectangular plate is an important structural component that is widely applied in various modern engineering fields, such as aircraft wings, rigid pavements, houses, and bridge decks. Bending analysis of a rectangular plate with mixed boundary conditions has been studied for many years, but most existing methods are appropriate only for particular boundary conditions. This study has changed miraculous attention due to the wide application of the rectangular plate.

Manthena et al. [1, 2] studied the temperature distribution, bending moments and thermal stresses in a functionally graded rectangular plate under unsteady temperature distribution using integral transform method. Manthena et al. [3]

*Corresponding author
Email addresses: drkr.gaikwad@yahoo.in (Kishor R. Gaikwad), ynaner@gmail.com (Yogesh U. Naner), khavalesatish8@gmail.com (Satish G. Khavale)

Received: March 2021 *Accepted:* September 2022

analyzed nonlinear thermo mechanical transverse deflection responses of the functionally graded curved structure under the influence of nonlinear thermal field. Amirpour et al. [4] developed a new analytical solution for elastic deformation of thin rectangular functionally graded plates with in-plane stiffness variation. Manthena et al. [5] determined the temperature distribution and thermal stresses of a thin rectangular plate. Tash et al. [6] studied the bending solution of simply supported transversely isotropic thick rectangular plates with thickness variations. Baghdasaryan et al. [7] investigated the stability of a rectangular plate in a supersonic flow in the presence of a temperature field. Xiao et al. [8] derived the governing equations of coupled thermoelasticity in a transversely vibrating rectangular plate by the modified nonlocal strain gradient theory and the nonlocal heat conductive law. Bajpai et al. [9] determined the effect of variable thermal conductivity and diffusivity on the transient response of thermoelastic diffusion plate in the light of two-temperature fractional-order generalized thermoelasticity. Peiyi et al. [10] investigated the convective heat transfer pattern of molten phase change material in a slender rectangular cavity with constant heat flux boundary condition. Ghasemi et al. [11] investigated the influences of thermophoresis and Brownian motion on thermo-hydraulic behavior of nanofluids in a sinusoidal wavy channel. Mahakalkar et al. [12] proposed the thermoelastic analysis of annular sector plate under restricted boundaries amidst elastic reaction. Jing-yi Liu et al. [12] analysed the effect of uniform laser irradiation on thermal response of temperature sensitive structures. Miao Wang et al. [14] discussed the buckling and free vibration analysis of shear deformable graphene-reinforced composite laminated plates. Nguyen Thi, et al. [15] analysed the nonlinear buckling of higher-order shear deformable stiffened FG-GRC laminated plates with nonlinear elastic foundation subjected to combined loads.

Ghasemi et al. [16] studied the thermohydraulic behavior of a thin liquid film on an unstable stretching surface under the influences of solar radiation and a porous medium. Ghasemi et al. [17] used the Joule heating and viscous dissipation properties to investigate the influences of magnetic field and nonlinear radiation on stagnation-point flow of nanofluid. Ghasemi et al. [18] discussed the vibration and frequency of single-walled carbon nanotubes with conveyance a fluid flow. Ghugal et al. [19] considered the effect of transverse shear and normal strain for the static analysis of laminated composite spherical shells subjected to sinusoidal mechanical/thermal loads with simply supported boundary conditions. Deepak et al. [20] discussed the analytical solution of a layered thin magneto-electro-elastic rectangular plate and produced the effect of transverse elastic boundary condition on the thickness variation of electric and magnetic potential under linear and moderately large deflection. Zahran et al. [21] investigated the turbulent air flow through a rectangular cross-sectional duct with one corrugated surface. Mohsenian et al. [22] studied the problem of convective heat transfer for a nanofluid flow between two tubes in the presence of a horizontal magnetized field. Gouran et al. [23] analyzed the thermal radiation on nanofluid flow between two circular cylinders under influence of magnetic field using two effectual computational methods. Gouran et al. [24] investigated the mixed convection and radiation heat transfer for a longitudinal fin with a constant velocity and considering heat source. Some contributors to this theory are the work in [25, 26, 27, 28, 29, 30, 31, 32, 33, 34, 35, 36, 37, 38, 39].

The solution of partial differential equations of heat conduction by the classical method of separation of variables is not always convenient when the equation and the boundary conditions involve non-homogeneities. It is for this reason that we considered the Green's function approach for the solution of linear, nonhomogeneous boundary value problems of heat conduction. The integral transform technique also provides a systematic, efficient, and straightforward approach for the solution of both homogeneous and nonhomogeneous, steady-state, and time-dependent boundary value problems of heat conduction.

According to the review of previous studies mentioned above, the research gap and objectives are described comprehensively as follows. Howbeit many mathematical analyses have been done on integral transform technique in the open literature, there is a gap in the simultaneously use of Green's function approach and integral transform technique for solving the thermal bending problem of rectangular plate with simply supported edge. The analytical solution of the rectangular plate with simply supported edge will be utilized for solving the issue. This is the main motivation behind this computational study, which will be very helpful in recovering some research gap in this field. Another novelty of our present work is to evaluate the accuracy of these methods to obtain analytic solutions and compare them with each other.

It is believed that, this particular problem has not been considered by any one. This is a new and novel contribution to the field of thermoelasticity. The results presented here will be more useful in engineering problems particularly, in the determination of the state of strain in circular plate constituting foundations of containers for hot gases or liquids, in the foundations for furnaces, etc. To verify the accuracy and validity of the approach, numerical results are presented for an easy comparison with those found in the literatures [1, 2, 3].

2 Basic Relations and Thermal Bending

The equation of equilibrium state:

$$N_x = N_y = N_{xy} = 0 \tag{1}$$

Bending moments:

$$M_x = \int_0^c \sigma_{xx} z dz \qquad M_y = \int_0^c \sigma_{yy} z dz \qquad M_{xy} = -\int_0^c \sigma_{xy} z dz \tag{2}$$

The equation of equilibrium in terms of moments as defined in [40].

$$\frac{\partial^2 M_x}{\partial x^2} - 2\frac{\partial^2 M_{xy}}{\partial x \partial y} + \frac{\partial^2 M_y}{\partial y^2} + p = 0 \tag{3}$$

where p denoted distributed external load.

The resultant moments as [40]:

$$\begin{aligned} M_x &= -D(\omega_{xx} + \nu\omega_{yy}) - \frac{1}{1-\nu} M_T \\ M_y &= -D(\omega_{yy} + \nu\omega_{xx}) - \frac{1}{1-\nu} M_T \\ M_{xy} &= (1-\nu) D\omega_{xy} \end{aligned} \tag{4}$$

where ν– Poisson's ratio, D– flexural rigidity.

$$D = \frac{Eh^3}{12(1-\nu^2)}$$

and the N_T– thermally induced resultant force, M_T– thermally induced resultant moment

$$N_T = \alpha E \int_0^c (T - T_0) dz, \quad M_T = \alpha E \int_0^c (T - T_0) z dz \tag{5}$$

where E–Young's modulus and α– linear coefficient of thermal expansion.

Stress components as [40]

$$\begin{aligned} \sigma_{xx} &= \frac{1}{h} N_x + \frac{12z}{h^3} M_x + \frac{1}{(1-\nu)} \left[\frac{1}{h} N_T + \frac{12z}{h^3} M_T - \alpha E (T - T_0) \right] \\ \sigma_{yy} &= \frac{1}{h} N_y + \frac{12z}{h^3} M_y + \frac{1}{(1-\nu)} \left[\frac{1}{h} N_T + \frac{12z}{h^3} M_T - \alpha E (T - T_0) \right] \\ \sigma_{xy} &= \frac{1}{h} N_{xy} - \frac{12z}{h^3} M_{xy} \end{aligned} \tag{6}$$

The equations of equilibrium in bending moments as

$$\begin{aligned} \frac{\partial M_x}{\partial x} + \frac{\partial M_{yx}}{\partial y} &= Q_x \\ \frac{\partial M_y}{\partial y} + \frac{\partial M_{xy}}{\partial x} &= Q_y \end{aligned} \tag{7}$$

where Q_x and Q_y are the shearing forces defined as

$$Q_x = \int_0^c \sigma_{xz} dz \qquad Q_y = \int_0^c \sigma_{yz} dz \qquad M_{yx} = \int_0^c \sigma_{yx} z dz \tag{8}$$

Putting Eqs. (4) in Eq. (3), one can easily obtain:

$$\frac{\partial^2}{\partial x^2} \left[D(\omega_{xx} + \nu\omega_{yy}) \right] + \frac{\partial^2}{\partial y^2} \left[D(\omega_{yy} + \nu\omega_{xx}) \right] + 2(1-\nu) \frac{\partial^2}{\partial x \partial y} (D\omega_{xy}) = p - \frac{1}{1-\nu} \nabla^2 M_T \tag{9}$$

Which is the fundamental equation of the bending of the plate due to the thermal load.

If the flexural rigidity D is not changed over the entire region of the plate, the fundamental equation Eq. (9) becomes

$$\nabla^2\nabla^2\omega = \frac{1}{D}\left(p - \frac{1}{(1-\nu)}\nabla^2 M_T\right) \tag{10}$$

where

$$\nabla^2 = \frac{\partial^2}{\partial x^2} + \frac{\partial^2}{\partial y^2} + \frac{\partial^2}{\partial z^2}$$

If the distributed external load p is absent then the Eq. (10) becomes

$$\nabla^2\nabla^2\omega = \frac{-1}{D(1-\nu)}\nabla^2 M_T \tag{2.1}$$

3 Problem Formulation

A rectangular thin plate and its coordinate system are illustrated in Figure 1. The plate's length, width, and thickness are a, b and c respectively. Initially, the plate is kept at a constant temperature. For $t > 0$, the heat is produced in the plate at the rate g (W.m^{-3}) and the surfaces at $x = 0, a$ and $y = 0, b$ kept at zero temperature, while the surfaces $z = 0, c$ are subjected to heat convection.

The differential equation for the temperature is

$$\frac{\partial^2 T}{\partial x^2} + \frac{\partial^2 T}{\partial y^2} + \frac{\partial^2 T}{\partial z^2} + \frac{g}{k_t} = \frac{1}{\alpha}\frac{\partial T}{\partial t} \tag{12}$$

with

$$\begin{aligned} T &= T_0 && \text{at } t = 0 \\ T &= 0 && \text{at } x = 0, a \\ T &= 0 && \text{at } y = 0, b \\ -k_t\frac{\partial T}{\partial z} &= h_c[T - T_\infty] && \text{at } z = 0 \\ k_t\frac{\partial T}{\partial z} &= h_c[T - T_\infty] && \text{at } z = c \end{aligned} \tag{13}$$

where k_t its thermal conductivity, $\alpha = k_t/\rho c$ its thermal diffusivity with ρ and c_p denoting the density and specific heat. The quantity $g(x, y, z, t) = g_i(t)\delta(x - x_0)\delta(y - y_0)\delta(z - z_0)$ represents heat source, where g_i instantaneous heat source, δ is a Dirac delta function that describe the heat source at a point (x_0, y_0, z_0).

Figure 1 shows the thin rectangular plate under simply supported edges under thermal load. The fundamental Eq. (2.1) and boundary conditions along x and y direction in [40]

$$\begin{aligned} \omega = 0, \omega_{xx} &= -\frac{1}{(1-\nu)D}M_T \quad \text{on } x = 0, a \\ \omega = 0, \omega_{yy} &= -\frac{1}{(1-\nu)D}M_T \quad \text{on } y = 0, b \end{aligned} \tag{14}$$

Now, the fundamental Eq. (2.1) is resolved into the following two equation system

$$\begin{aligned} \nabla^2\omega + \frac{1}{(1-\nu)D}M_T &= F \\ \nabla^2 F &= 0 \end{aligned} \tag{15}$$

Thus, Eq. (15) is the governing equation for an unknown function F and Eq. (14) is recognized as a boundary condition for F.

$$F = \omega_{xx} + \omega_{yy} + \frac{1}{(1-\nu)D}M_T \tag{16}$$

We find that the curvature along the boundary surface becomes equal to zero

$$\begin{aligned} \omega_{yy} &= 0 \quad \text{on } x = 0, a \\ \omega_{xx} &= 0 \quad \text{on } y = 0, b \end{aligned} \tag{17}$$

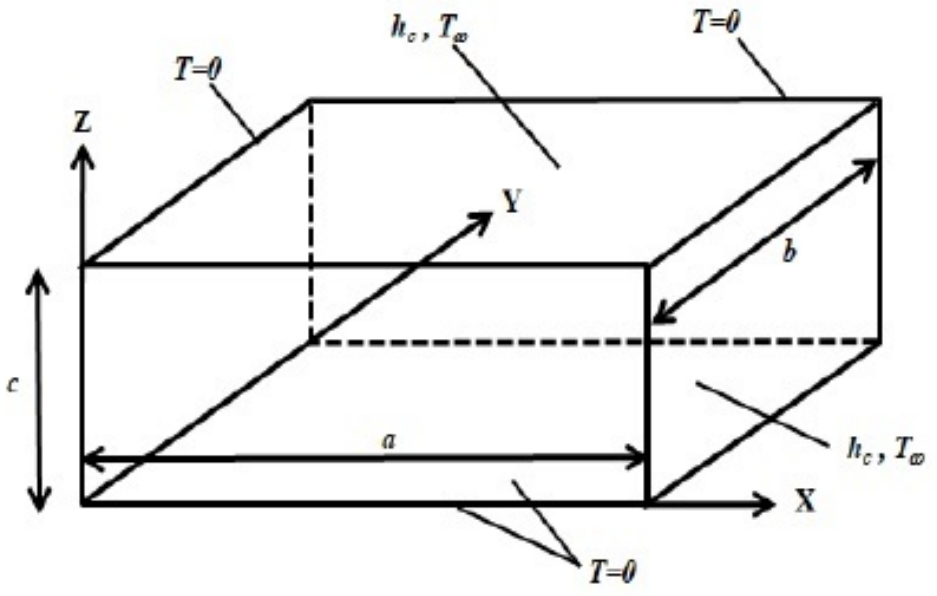

Figure 1: Problem Geometry.

Using Eqs. (16) and (17), the conditions Eq. (14) are reduced to the boundary conditions for F

$$\begin{aligned} F &= 0 \quad \text{on } x = 0, a \\ F &= 0 \quad \text{on } y = 0, b \end{aligned} \tag{18}$$

Therefore, the fundamental equation system given by Eqs. (15) and (18) is equal to zero.

$$F = 0 \tag{19}$$

Using Eq. (19) in Eq. (15), the governing equation for a simply supported rectangular plate is

$$\nabla^2 \omega = -\frac{1}{(1-\nu)D} M_T \tag{20}$$

with

$$\begin{aligned} \omega &= 0 \quad \text{on } x = 0, a \\ \omega &= 0 \quad \text{on } y = 0, b \end{aligned} \tag{21}$$

4 Solution of the problem

First, we modified the formulated BVP with the homogeneous boundary conditions. The temperature $T(t; x, y, z) = \Psi(t; x, y, z) + T_\infty$, where the constant ambient component T_∞ satisfies Eq. (12) and the dynamic component Ψ satisfies the following equations:

$$\frac{\partial^2 \Psi}{\partial x^2} + \frac{\partial^2 \Psi}{\partial y^2} + \frac{\partial^2 \Psi}{\partial z^2} + \frac{g(t; x, y, z)}{k_t} = \frac{1}{\alpha} \frac{\partial \Psi}{\partial t} \tag{22}$$

The initial and boundary conditions (13) becomes

$$\begin{aligned} \Psi &= T_0 - T_\infty \qquad \text{at } t = 0 \\ \Psi &= 0 \qquad \text{at } x = 0, a \\ \Psi &= 0 \qquad \text{at } y = 0, b \\ -\frac{\partial \Psi}{\partial z} + h_{s1} \Psi &= 0 \qquad \text{at } z = 0 \\ \frac{\partial \Psi}{\partial z} + h_{s2} \Psi &= 0 \qquad \text{at } z = c \end{aligned} \tag{23}$$

where $h_{s1} = h_c/k_t$, $h_{s2} = h_c/k_t$ are the coefficients of heat transfer.

Consider the homogeneous form of Eq. (22) with $g(t; x, y, z) = 0$,

$$\frac{\partial^2 \Psi}{\partial x^2} + \frac{\partial^2 \Psi}{\partial y^2} + \frac{\partial^2 \Psi}{\partial z^2} = \frac{1}{\alpha}\frac{\partial \Psi}{\partial t} \tag{24}$$

The initial and boundary conditions (23) becomes

$$\begin{aligned} \Psi &= T_0 - T_\infty \qquad \text{at } t = 0 \\ \Psi &= 0 \qquad\qquad\quad \text{at } x = 0, a \\ \Psi &= 0 \qquad\qquad\quad \text{at } y = 0, b \\ -\frac{\partial \Psi}{\partial z} &+ h_{s1}\Psi = 0 \qquad \text{at } z = 0 \\ \frac{\partial \Psi}{\partial z} &+ h_{s2}\Psi = 0 \qquad \text{at } z = c \end{aligned} \tag{25}$$

We define the integral transform and its inversion as [41]:

$$\begin{pmatrix}\text{Triple-integral}\\ \text{Transform}\end{pmatrix} \overline{\overline{\overline{\Psi}}}(t; \beta_m, \gamma_n, \eta_p) = \int_{x'=0}^{a}\int_{y'=0}^{b}\int_{z'=0}^{c} \frac{K_0(\beta_m, x').K_1(\gamma_n, y').K_2(\eta_p, z')}{S(\beta_m)S(\gamma_n)S(\eta_p)} \times \Psi(t; x', y', z').dx'dy'dz' \tag{26}$$

$$\begin{pmatrix}\text{Triple-inversion}\\ \text{formula}\end{pmatrix} \Psi(t; x, y, z) = \sum_{m=0}^{\infty}\sum_{n=0}^{\infty}\sum_{p=0}^{\infty} K_0(\beta_m, x).K_1(\gamma_n, y).K_2(\eta_p, z).\overline{\overline{\overline{\Psi}}}(t; \beta_m, \gamma_n, \eta_p) \tag{27}$$

where

$$K_0(\beta_m, x) = \sin \beta_m x, \qquad S(\beta_m) = \frac{a}{2}, \qquad \sin \beta_m a = 0$$

$$K_1(\gamma_n, y) = \sin \gamma_n y, \qquad S(\gamma_n) = \frac{b}{2}, \qquad \sin \gamma_n b = 0$$

$$K_2(\eta_p, z) = \eta_p \cos \eta_p z + h_{s1} \sin \eta_p z, \qquad S(\eta_p) = \frac{A_1}{2}, \qquad \tan \eta_p c = \frac{\eta_p(h_{s1} + h_{s2})}{\eta_p^2 - h_{s1}h_{s2}}$$

where $A_1 = \left[(\eta_p^2 + h_{s1}^2)\left(c + \frac{h_{s2}}{\eta_p^2 + h_{s2}^2}\right) + h_{s1}\right]$.

Applying the transforms defined in Eqs. (26–27) on Eq. (24)–(25), one obtains

$$\Psi(t; x, y, z) = \sum_{m=1}^{\infty}\sum_{n=1}^{\infty}\sum_{p=1}^{\infty} \frac{K_0(\beta_m, x).K_1(\gamma_n, y).K_2(\eta_p, z)}{S(\beta_m)S(\gamma_n)S(\eta_p)}.\exp(-\alpha\lambda_{mnp}^2 t).\overline{\overline{\overline{F}}}(\beta_m, \gamma_n, \eta_p) \tag{28}$$

where

$$\overline{\overline{\overline{F}}}(\beta_m, \gamma_n, \eta_p) = \int_{x'=0}^{a}\int_{y'=0}^{b}\int_{z'=0}^{c} K_0(\beta_m, x').K_1(\gamma_n, y').K_2(\eta_p, z')(T_0 - T_\infty)dx'dy'dz'$$

$$\lambda_{mnp}^2 = \beta_m^2 + \gamma_n^2 + \eta_p^2$$

The function Ψ can be written in the form of Green's function approach [41]:

$$\Psi(t; x, y, z) = \int_{x'=0}^{a}\int_{y'=0}^{b}\int_{z'=0}^{c} G(t; x, y, z, \mid \tau; x', y', z') \mid_{\tau=0} (T_0 - T_\infty)dx'dy'dz' \tag{29}$$

The Green's function as:

$$G(x, y, z, t \mid x', y', z', \tau) = \sum_{m=1}^{\infty}\sum_{n=1}^{\infty}\sum_{p=1}^{\infty} \frac{K_0(\beta_m, x).K_1(\gamma_n, y).K_2(\eta_p, z)}{S(\beta_m)S(\gamma_n)S(\eta_p)} \times K_0(\beta_m, x').K_1(\gamma_n, y').K_2(\eta_p, z')\exp(-\alpha\lambda_{mnp}^2 t) \tag{30}$$

Finally, the solution of nonhomogeneous problems of Eqs. (12) and (13) as:

$$\begin{aligned} T(t; x, y, z) = T_\infty &+ \int_{x'=0}^{a}\int_{y'=0}^{b}\int_{z'=0}^{c} G(t; x, y, z \mid \tau; x', y', z') \mid_{\tau=0} (T_0 - T_\infty)dx'dy'dz' \\ &+ \frac{\alpha}{k_t}\int_{\tau=0}^{t}\int_{x'=0}^{a}\int_{y'=0}^{b}\int_{z'=0}^{c} G(t; x, y, z \mid \tau; x', y', z').g(\tau; x', y', z',)dx'dy'dz'd\tau. \end{aligned} \tag{31}$$

4.1 Special Case:

Setting, $T_0 = T_\infty$ and $g(t;x,y,z) = 1(t)\delta(x-x_0)(y-y_0)(z-z_0)$ with $1(t)$ denoting a unit step function in Eq. (31), the temperature distribution becomes

$$T(t;x,y,z) = T_0 + \frac{1}{k_t}\sum_{m=1}^{\infty}\sum_{n=1}^{\infty}\sum_{p=1}^{\infty}\frac{K_0(\beta_m,x).K_1(\gamma_n,y).K_2(\eta_p,z)}{S(\beta_m)S(\gamma_n)S(\eta_p)} \times K_0(\beta_m,x_0).K_1(\gamma_n,y_0).K_2(\eta_p,z_0)\left[\frac{1-\exp(-\alpha\lambda_{mnp}^2 t)}{\lambda_{mnp}^2}\right] \tag{32}$$

4.2 Thermally Induced Resultant Force and Resultant Moment:

Using Eq. (32) in Eq. (5), we obtain

$$N_T = \frac{\alpha E}{k_t}\sum_{m=1}^{\infty}\sum_{n=1}^{\infty}\sum_{p=1}^{\infty}\frac{K_0(\beta_m,x).K_1(\gamma_n,y)}{S(\beta_m)S(\gamma_n)S(\eta_p)}\left[\sin\eta_p c + \frac{h_{s1}}{\eta_p}(1-\cos\eta_p c)\right] \times K_0(\beta_m,x_0).K_1(\gamma_n,y_0).K_2(\eta_p,z_0)\left[\frac{1-\exp(-\alpha\lambda_{mnp}^2 t)}{\lambda_{mnp}^2}\right] \tag{33}$$

$$M_T = \frac{\alpha E}{k_t}\sum_{m=1}^{\infty}\sum_{n=1}^{\infty}\sum_{p=1}^{\infty}\frac{K_0(\beta_m,x).K_1(\gamma_n,y)}{S(\beta_m)S(\gamma_n)S(\eta_p)}\left[\left(c+\frac{h_{s1}}{\eta_p}\right)\sin\eta_p c + \left(\frac{1}{\eta_p}-\frac{h_{s1}}{\eta_p}\right)\cos\eta_p c - \frac{1}{\eta_p}\right] \times K_0(\beta_m,x_0).K_1(\gamma_n,y_0).K_2(\eta_p,z_0)\left[\frac{1-\exp(-\alpha\lambda_{mnp}^2 t)}{\lambda_{mnp}^2}\right] \tag{34}$$

4.3 The Thermal Deflection:

Using Eq. (34) in Eq. (20), we obtain

$$\omega(x,y) = \frac{\alpha E}{(1-\nu)Dk_t}\sum_{m=1}^{\infty}\sum_{n=1}^{\infty}\sum_{p=1}^{\infty}\frac{1}{(\beta_m^2+\gamma_n^2)}\frac{K_0(\beta_m,x).K_1(\gamma_n,y)}{S(\beta_m)S(\gamma_n)S(\eta_p)} \times\left[\left(c+\frac{h_{s1}}{\eta_p}\right)\sin\eta_p c + \left(\frac{1}{\eta_p}-\frac{h_{s1}}{\eta_p}\right)\cos\eta_p c - \frac{1}{\eta_p}\right] \times K_0(\beta_m,x_0).K_1(\gamma_n,y_0).K_2(\eta_p,z_0)\left[\frac{1-\exp(-\alpha\lambda_{mnp}^2 t)}{\lambda_{mnp}^2}\right] \tag{35}$$

4.4 The resultant moments:

Using Eqs. (34) and (35) in Eq. (4), we obtain

$$M_x = \frac{-\alpha E}{k_t}\sum_{m=1}^{\infty}\sum_{n=1}^{\infty}\sum_{p=1}^{\infty}\frac{\gamma_n^2}{(\beta_m^2+\gamma_n^2)}\frac{K_0(\beta_m,x).K_1(\gamma_n,y)}{S(\beta_m)S(\gamma_n)S(\eta_p)} \times\left[\left(c+\frac{h_{s1}}{\eta_p}\right)\sin\eta_p c + \left(\frac{1}{\eta_p}-\frac{h_{s1}}{\eta_p}\right)\cos\eta_p c - \frac{1}{\eta_p}\right] \times K_0(\beta_m,x_0).K_1(\gamma_n,y_0).K_2(\eta_p,z_0)\left[\frac{1-\exp(-\alpha\lambda_{mnp}^2 t)}{\lambda_{mnp}^2}\right] \tag{36}$$

$$M_y = \frac{-\alpha E}{k_t}\sum_{m=1}^{\infty}\sum_{n=1}^{\infty}\sum_{p=1}^{\infty}\frac{\beta_m^2}{(\beta_m^2+\gamma_n^2)}\frac{K_0(\beta_m,x).K_1(\gamma_n,y)}{S(\beta_m)S(\gamma_n)S(\eta_p)} \times\left[\left(c+\frac{h_{s1}}{\eta_p}\right)\sin\eta_p c + \left(\frac{1}{\eta_p}-\frac{h_{s1}}{\eta_p}\right)\cos\eta_p c - \frac{1}{\eta_p}\right] \times K_0(\beta_m,x_0).K_1(\gamma_n,y_0).K_2(\eta_p,z_0)\left[\frac{1-\exp(-\alpha\lambda_{mnp}^2 t)}{\lambda_{mnp}^2}\right] \tag{37}$$

$$M_{xy} = \frac{\alpha E}{k_t}\sum_{m=1}^{\infty}\sum_{n=1}^{\infty}\sum_{p=1}^{\infty}\frac{\beta_m\gamma_n}{(\beta_m^2+\gamma_n^2)}\frac{\cos\beta_m x.\cos\gamma_n y}{S(\beta_m)S(\gamma_n)S(\eta_p)} \times\left[\left(c+\frac{h_{s1}}{\eta_p}\right)\sin\eta_p c+\left(\frac{1}{\eta_p}-\frac{h_{s1}}{\eta_p}\right)\cos\eta_p c-\frac{1}{\eta_p}\right] \times K_0(\beta_m,x_0).K_1(\gamma_n,y_0).K_2(\eta_p,z_0)\left[\frac{1-\exp(-\alpha\lambda_{mnp}^2 t)}{\lambda_{mnp}^2}\right] \tag{38}$$

4.5 The thermal stresses:

Using Eqs. (32), (33)–(34) and (36)–(38) in Eq. (6), we obtain

$$\begin{aligned}\sigma_{xx} = &\left\{\frac{12z}{c^3}\left(\frac{-\alpha E}{k_t}\sum_{m=1}^{\infty}\sum_{n=1}^{\infty}\sum_{p=1}^{\infty}\frac{\gamma_n^2}{(\beta_m^2+\gamma_n^2)}\frac{K_0(\beta_m,x).K_1(\gamma_n,y)}{S(\beta_m)S(\gamma_n)S(\eta_p)}\right.\right.\\ &\times\left[\left(c+\frac{h_{s1}}{\eta_p}\right)\sin\eta_p c+\left(\frac{1}{\eta_p}-\frac{h_{s1}}{\eta_p}\right)\cos\eta_p c-\frac{1}{\eta_p}\right]\Big)\\ &+\frac{1}{c(1-\nu)}\left(\frac{\alpha E}{k_t}\sum_{m=1}^{\infty}\sum_{n=1}^{\infty}\sum_{p=1}^{\infty}\frac{K_0(\beta_m,x).K_1(\gamma_n,y)}{S(\beta_m)S(\gamma_n)S(\eta_p)}\left[\sin\eta_p c+\frac{h_{s1}}{\eta_p}(1-\cos\eta_p c)\right]\right)\\ &+\frac{12z}{c^3(1-\nu)}\left(\frac{\alpha E}{k_t}\sum_{m=1}^{\infty}\sum_{n=1}^{\infty}\sum_{p=1}^{\infty}\frac{K_0(\beta_m,x).K_1(\gamma_n,y)}{S(\beta_m)S(\gamma_n)S(\eta_p)}\right.\\ &\times\left[\left(c+\frac{h_{s1}}{\eta_p}\right)\sin\eta_p c+\left(\frac{1}{\eta_p}-\frac{h_{s1}}{\eta_p}\right)\cos\eta_p c-\frac{1}{\eta_p}\right]\Big)\\ &\left.\left.-\frac{\alpha E}{(1-\nu)}\left(\frac{1}{k_t}\sum_{m=1}^{\infty}\sum_{n=1}^{\infty}\sum_{p=1}^{\infty}\frac{K_0(\beta_m,x).K_1(\gamma_n,y).K_2(\eta_p,z)}{S(\beta_m)S(\gamma_n)S(\eta_p)}\right)\right\}\\ &\times K_0(\beta_m,x_0).K_1(\gamma_n,y_0).K_2(\eta_p,z_0)\left[\frac{1-\exp(-\alpha\lambda_{mnp}^2 t)}{\lambda_{mnp}^2}\right]\end{aligned} \tag{39}$$

$$\begin{aligned}\sigma_{yy} = &\left\{\frac{12z}{c^3}\left(\frac{-\alpha E}{k_t}\sum_{m=1}^{\infty}\sum_{n=1}^{\infty}\sum_{p=1}^{\infty}\frac{\beta_m^2}{(\beta_m^2+\gamma_n^2)}\frac{K_0(\beta_m,x).K_1(\gamma_n,y)}{S(\beta_m)S(\gamma_n)S(\eta_p)}\right.\right.\\ &\times\left[\left(c+\frac{h_{s1}}{\eta_p}\right)\sin\eta_p c+\left(\frac{1}{\eta_p}-\frac{h_{s1}}{\eta_p}\right)\cos\eta_p c-\frac{1}{\eta_p}\right]\Big)\\ &+\frac{1}{c(1-\nu)}\left(\frac{\alpha E}{k_t}\sum_{m=1}^{\infty}\sum_{n=1}^{\infty}\sum_{p=1}^{\infty}\frac{K_0(\beta_m,x).K_1(\gamma_n,y)}{S(\beta_m)S(\gamma_n)S(\eta_p)}\left[\sin\eta_p c+\frac{h_{s1}}{\eta_p}(1-\cos\eta_p c)\right]\right)\\ &+\frac{12z}{c^3(1-\nu)}\left(\frac{\alpha E}{k_t}\sum_{m=1}^{\infty}\sum_{n=1}^{\infty}\sum_{p=1}^{\infty}\frac{K_0(\beta_m,x).K_1(\gamma_n,y)}{S(\beta_m)S(\gamma_n)S(\eta_p)}\right.\\ &\times\left[\left(c+\frac{h_{s1}}{\eta_p}\right)\sin\eta_p c+\left(\frac{1}{\eta_p}-\frac{h_{s1}}{\eta_p}\right)\cos\eta_p c-\frac{1}{\eta_p}\right]\Big)\\ &\left.\left.-\frac{\alpha E}{(1-\nu)}\left(\frac{1}{k_t}\sum_{m=1}^{\infty}\sum_{n=1}^{\infty}\sum_{p=1}^{\infty}\frac{K_0(\beta_m,x).K_1(\gamma_n,y).K_2(\eta_p,z)}{S(\beta_m)S(\gamma_n)S(\eta_p)}\right)\right\}\\ &\times K_0(\beta_m,x_0).K_1(\gamma_n,y_0).K_2(\eta_p,z_0)\left[\frac{1-\exp(-\alpha\lambda_{mnp}^2 t)}{\lambda_{mnp}^2}\right]\end{aligned} \tag{40}$$

$$\sigma_{xy} = -\frac{12z}{c^3}\left\{\frac{\alpha E}{k_t}\sum_{m=1}^{\infty}\sum_{n=1}^{\infty}\sum_{p=1}^{\infty}\frac{\beta_m\gamma_n}{(\beta_m^2+\gamma_n^2)}\frac{\cos\beta_m x.\cos\gamma_n y}{S(\beta_m)S(\gamma_n)S(\eta_p)}\right.$$
$$\times\left[\left(c+\frac{h_{s1}}{\eta_p}\right)\sin\eta_p c+\left(\frac{1}{\eta_p}-\frac{h_{s1}}{\eta_p}\right)\cos\eta_p c-\frac{1}{\eta_p}\right] \tag{41}$$
$$\left.\times K_0(\beta_m,x_0).K_1(\gamma_n,y_0).K_2(\eta_p,z_0)\left[\frac{1-\exp(-\alpha\lambda_{mnp}^2 t)}{\lambda_{mnp}^2}\right]\right\}$$

5 Results and discussion

For numerical calculation, we choose copper material with following physical constants as illustrated in Table 1.

Table 1: Material constants

$\rho = 8954$ kg/m^3	$\alpha = 112.34(10)^{-6}$ m^2/s	$k_t = 386$ W/(m K)
E = 128 Gpa	$c_p = 383$ J/(kg K)	$a_t = 16.5(10)^{-6}$ K^{-1}
$\nu = 0.35$	μ =26.67	g_i= 200 W/m^3
$h_{s1} = 10$, $h_{s2} = 0$	$a = 1$ m, $b = 0.5$ m	$c = 0.1$ m, $T_0 = 0$ K

5.1 Roots of the Transcendental Equation

Here $\beta_1 = 6.28$, $\beta_2 = 12.56$, $\beta_3 = 18.84$, $\beta_4 = 25.12$, $\beta_5 = 31.40$ are the positive root of

$$\sin\beta_m a = 0$$

and $\eta_1 = 1.4289$, $\eta_2 = 4.3058$, $\eta_3 = 7.2281$, $\eta_4 = 10.2003$, $\eta_5 = 13.2142$ are the positive roots of

$$\tan(\eta c) = \frac{\eta(h_{s1}+h_{s2})}{\eta^2 - h_{s1}h_{s2}}$$

has the form $\eta\tan(\eta) = c$, for $c = 1$, $h_{s1} = c = 10$, $h_{s2} = 0$ in [41]. The numerical calculations have been presented by the PTC MATHCAD (Prime-3.1) and the results are depicted graphically.

Notice that

$$\beta_m = \gamma_n = \eta_p \to \infty \qquad \text{as} \quad m,n,p \to \infty$$
$$e^{-k\beta_m^2.t} = e^{-k\gamma_n^2.t} = e^{-k\eta_p^2.t} \to 0 \qquad \text{as} \quad m,n,p \to \infty.$$

The terms $\sin(\beta_m x)$ and $\cos(\beta_m x)$ are bounded.

The conditions of convergence are verified by the D-Alemberts ratio test. Hence, all the series in (32) to (41) are convergent. For a large value of m, n, and p the expression for displacement, temperature, and stress fields are negligible and it converges to zero at infinity. For the purpose of numerical calculations, the number of terms is used in Fourier are chosen to be $m = n = p = 50$. It is assumed that the plate is subject to an instantaneous point heat source of strength $g_i = 200$ W/m, situated at the middle part of the plate with initially at zero temperature i.e. $T_0(x, y, z) = 0$

This section presents numerical results of temperature, thermal deflection and stresses profiles for different parameters.

The effect of time parameters on distribution of the temperature profile is depicted in Figure 2. It is seen that the magnitude of temperature is gradually increasing with an increase in time and it attains it peak at $x = 0.5$, after that it gradually decreasing with an increase in time, which is according to the boundary conditions.

Figure 3, demonstrates the efficacy of time parameters on deflection profile along the distance X. We observe that, the magnitude of temperature is gradually increasing with an increase in time and it attains it peak at $x = 0.5$, after that it gradually decreasing with an increase in time, which is according to the boundary conditions. Due to

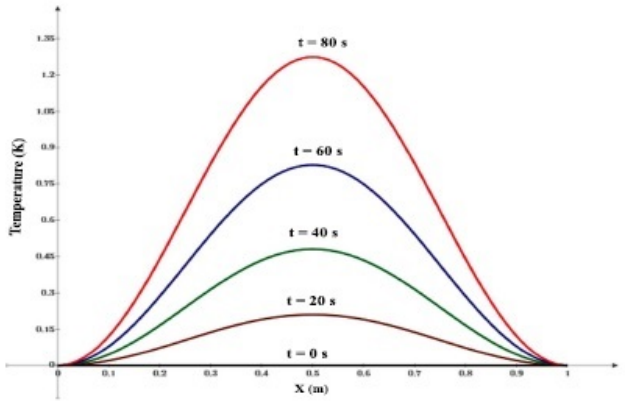

Figure 2: Temperature distribution.

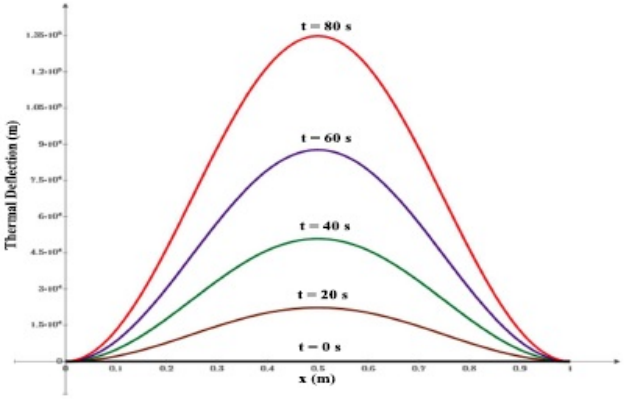

Figure 3: Thermal deflection.

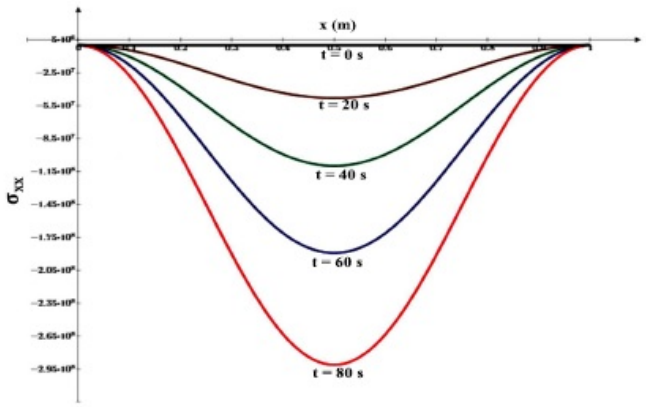

Figure 4: Stress distribution.

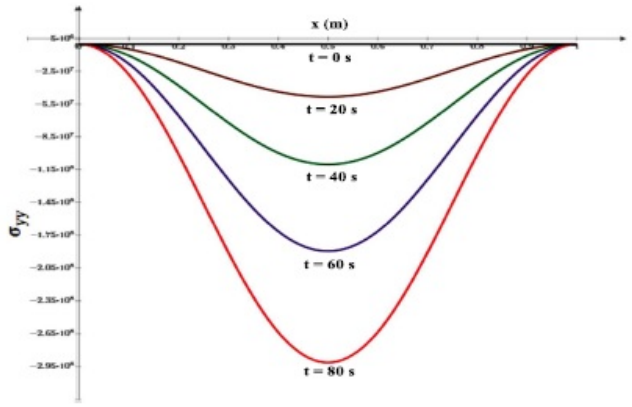

Figure 5: Stress distribution.

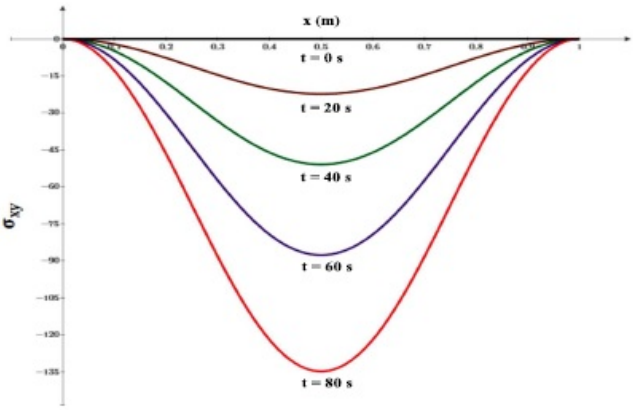

Figure 6: Stress distribution.

the instantaneous point heat source, the thermal deflection is maximum at the middle of the plate with increasing the time parameter and decreases towards the outer boundaries.

Figures 4, 5, and 6 predicts the variations of the stresses with respect to the distance X. We observe that the magnitude of all stresses is maximum at the middle part with increasing time and becomes zero at the origin and extreme edges in the X-direction. Also, the stress components σ_{xx}, σ_{yy}, and σ_{xy} are compressive throughout the plate.

Due to the instantaneous point heat source of strength $g_i = 200$ W/m, situated at the middle part of the plate, small deflection and deformation in the middle part of the plate. Due to contemptible amount of deflection, there will not be any personage crawl or shrinkage in solid.

6 Conclusion

In the present work, the Green's function approach and integral transform technique have been utilized to analyze the thermal bending problem of a rectangular plate with simply supported edge. The obtained results were evaluated to investigate the convective heat transfer coefficient as well as velocity and temperature for various physical parameters.

The important findings are summarized as follows:

1. By D-Alembert's ratio test, all the series in (32)–(41) are convergent.
2. The temperature profile and the thermal deflection are maximum at the middle part of the plate, due to the heat source located at the middle.
3. From the graph of temperature and deflection, it is clear that the direction heat of flow and the body deformation is the same. We conclude that the maximum heat occurs at the middle part of the plate, this is due to the heat source.
4. The temperature and deflection are proportionate to each other and it shows the normal curve.
5. The stresses σ_{xx}, σ_{yy}, and σ_{xy} develop the compressive stresses.
6. The Green's function approach and integral transform technique, are our most general and powerful method to solve nonhomogeneous, time-dependent conduction problems.
7. The simplicity and efficacy of these techniques to find analytical solutions are advantageous in heat transfer issues.
8. To improve the solution speed and better accuracy of the results, the proposed method offers an alternative for solving engineering problems.

To further study for this problem, consider a rectangular plate with built in all edges will be suggested. Varying the boundary condition to a variable heat flux also leads to a new inspiration to continue the current work.

Acknowledgment

This project was funded by the CSIR-HRDG, New Delhi, India under Grant [File No.: 08/581(0003)2017-EMR-I].

References

[1] V.R. Manthena, N.K. Lamba, G.D. Kedar and K.C. Deshmukh, *Effects of stress resultants on thermal stresses in a functionally graded rectangular plate due to temperature dependent material properties*, Int. J. Thermodyn. **19** (2016), no. 4, 235–242.

[2] V.R. Manthena, N.K. Lamba and G.D. Kedar, *Transient thermoelastic problem of a nonhomogeneous rectangular plate*, J. Thermal Stresses **40** (2017), no. 5, 627–640.

[3] T.R. Mahapatra, V.R. Kar, S.K. Panda and K. Mehar, *Nonlinear thermoelastic deflection of temperature-dependent FGM curved shallow shell under nonlinear thermal loading*, J. Thermal Stresses **40** (2017), no. 9, 1184–1199.

[4] M. Amirpour, R. Das and E.I. Saavedra Flores, *Bending analysis of thin functionally graded plate under in-plane stiffness variations*, Appl. Math. Model.**44** (2017), 481–496.

[5] V.R. Manthena, G.D. Kedar and K.C. Deshmukh, *Thermal stress analysis of a thermosensitive functionally graded rectangular plate due to thermally induced resultant moments*, Multidiscip. Model. Mater. Struct. **14** (2018), no. 5, . 857–873.

[6] F. Yekkalam Tash and B. Navayi Neya, *An analytical solution for bending of transversely isotropic thick rectangular plates with variable thickness*, Appl. Math. Model. **77** (2020), no. 2, 1582–1602.

[7] G.Y. Baghdasaryan, M.A. Mikilyan, I.A. Vardanyan, K.V. Melikyan and P. Marzocca, *Thermoelastic non-linear flutter oscillations of rectangular plate*, J. Thermal Stresses **44** (2021), no. 6, 731–754.

[8] Xiao Ge, Pu Li, Yuming Fang and Longfei Yang, *Thermoelastic damping in rectangular microplate/nanoplate resonators based on modified nonlocal strain gradient theory and nonlocal heat conductive law*, J. Thermal Stresses **44** (2021), no. 6, 690–714.

[9] Ankit Bajpai and P. K. Sharma, *Variable thermal conductivity and diffusivity impact on forced vibrations of thermodiffusive elastic plate*, J. Thermal Stresses **44** (2021), no. 9, . 1169–1190.

[10] P. Li , Z. Wang, Z. Liu, W. Heng and H. Qin, *Convective heat transfer mechanisms of molten phase change material in a vertical slender rectangular cavity: A numerical case study*, Case Stud. Thermal Engin. **26** (2021).

[11] S.E. Ghasemi, S. Gouran and A. Zolfagharian, *Thermal and hydrodynamic analysis of a conducting nanofluid flow through a sinusoidal wavy channel*, Case Stud. Thermal Engin. **28** (2021).

[12] A. Mahakalkar and V. Varghese, *Thermoelastic analysis of annular sector plate under restricted boundaries amidst elastic reaction*, J. Solid Mech. **13** (2021), no. 3, 325–337.

[13] J.-Yi Liu, L.-C. Long and C.-Y. Zhang, *Effect of uniform laser irradiation on thermal response of temperature sensitive structures*, AIP Adv. **11** (2021), 065107.

[14] M. Wang, Y.-G. Xu, P. Qiao and Z.-M. Li, *Buckling and free vibration analysis of shear deformable graphene-reinforced composite laminated plates*, Composite Struct. **280** (2022), no. 15, 114854.

[15] N. Thi, P. Dang, T. Dong, C. Van Doan and V. Hoai Nam, *Nonlinear buckling of higher-order shear deformable stiffened FG-GRC laminated plates with nonlinear elastic foundation subjected to combined loads*, Aerospace Sci. Technol. **127** (2022), 107736.

[16] S.E. Ghasemi and S. Gouran, *Theoretical incestigation of solar radiation on a thin liquid film over an unstable stretching sheet surrounded by a porous medium*, J. Porous Media. **25** (2022), no. 7, 89–100.

[17] S.E. Ghasemi, S. Mohsenian, S. Gouran and A. Zolfagharian, *A novel spectral relaxation approach for nanofluid flow past a stretching surface in presence of magnetic field and nonlinear radiation*, Results Phys. **32** (2022).

[18] S.E. Ghasemi and S. Gouran, *Nonlinear analysis on flow-induced vibration of single-walled carbon nanotubes employing analytical methods*, International J. Struct. Stab. Dyn. **22** (2022), no. 11, 2250115.

[19] Y.M. Ghugal, A.S. Sayyad and S.M. Girme, *Thermoelastic bending analysis of laminated composite shells using a trigonometric shear and normal deformation theory*, Journal of Thermal Stresses. **45** (2022), no. 3, 171–190.

[20] P. Deepak, K. Jayakumar and P. Satyananda, *Electromagnetic response of layered Magneto-Electro-Elastic thin rectangular plate under moderately large deflection*, Composites: Mech. Comput. Appl. **13** (2022), no. 1, 25–48.

[21] S. Zahran, A.A. Sultan, M. Bekheit and M.R. Elmarghany, *Heat transfer augmentation through rectangular cross section duct with one corrugated surface: An experimental and numerical study*, Case Studies Thermal Engin. **36** (2022).

[22] S. Mohsenian, S. Gouran and S.E. Ghasemi, *Evaluation of weighted residual methods for thermal radiation on nanofluid flow between two tubes in presence of magnetic field*, Case Stud. Thermal Engin. **32** (2022).

[23] S. Gouran, S. Mohsenian and S.E. Ghasemi, *Theoretical analysis on MHD nanofluid flow between two concentric cylinders using efficient computational techniques*, Alexandria Engin. J. **61** (2022), 3237–3248.

[24] S. Gouran, S.E. Ghasemi and S. Mohsenian, *Effect of internal heat source and non-independent thermal properties on a convective–radiative longitudinal fin*, Alexandria Engin. J. **61** (2022), 8545–8554.

[25] K.R. Gaikwad and K.P. Ghadle, *Quasi-static thermal stresses in a thick rectangular plate*, Global J. Pure Appl. Math. **5** (2009), no. 2, 109–117.

[26] K.R. Gaikwad and K.P. Ghadle, *Three dimensional non-homogeneous thermoelastic problem in a thick rectangular plate due to internal heat generation*, SAJPAM **5** (2011), 26–38.

[27] K.R. Gaikwad and K.P. Ghadle, *Nonhomogeneous heat conduction problem and its thermal deflection due to internal heat generation in a thin hollow circular disk*, J. Thermal Stresses **35** (2012), no. 6, 485–498.

[28] K.R. Gaikwad, *Analysis of thermoelastic deformation of a thin hollow circular disk due to partially distributed heat supply*, J. Thermal Stresses **36** (2013), no. 3, 207–224.

[29] K.R. Gaikwad, *Two-dimensional steady-state temperature distribution of a thin circular plate due to uniform internal energy generation*, Cogent Math.**3** (2016), no. 1, 1–10.

[30] K.R. Gaikwad, *Axi-symmetric thermoelastic stress analysis of a thin circular plate due to heat generation*, Int. J. Dyn. Syst. Differ. Equ. **9** (2019), 187–202.

[31] K.R. Gaikwad and S.G. Khavale, *Time fractional 2D thermoelastic problem of thin hollow circular disk and it's associated thermal stresses*, Bull. Marathwada Math. Soc. **21** (2020), no. 1-2, 37-–47.

[32] K.R. Gaikwad and Y.U. Naner, *Transient thermoelastic stress analysis of a thin circular plate due to uniform internal heat generation*, J. Korean Soc. Ind. Appl. Math. **24** (2020), no. 3, 293–303.

[33] K.R. Gaikwad and Y.U. Naner, *Analysis of transient thermoelastic temperature distribution of a thin circular plate and its thermal deflection under uniform heat generation*, J. Thermal Stresses **44** (2021), no. 1, 75–85.

[34] K.R. Gaikwad, Y.U. Naner and S.G. Khavale, *Time fraectional thermoelastic stress anlysis of a thin rectangular plate*, NOVYI MIR Res. J. **6** (2021), no. 1, 42–56.

[35] S.G. Khavale and K.R. Gaikwad, *Fractional Order Thermoelatic Problem of Thin Hollow Circular Disk and its Thermal Stresses Under Axi-Symmetric Heat Supply*, Design Engin. **12** (2021), no. 9,pp. 13851–13862.

[36] S.G. Khavale and K.R. Gaikwad, *Analysis of non-integer order thermoelastic temperature distribution and thermal deflection of a thin hollow circular disk under the axi-symmetric heat supply*, J. Korean Soc. Ind. Apll. Math. **26** (2022), no. 1, 67—75.

[37] K.R. Gaikwad and S.G. Khavale, *Fractional order transient thermoelastic stress analysis of a thin circular sector disk*, Int. J. Thermodyn. **25** (2022), no. 1, 1–8.

[38] S.G. Khavale and K.R. Gaikwad, *2D Problem for a Sphere in the Fractional Order Theory Thermoelasticity to Axisymmetric Temperature Distribution*, Adv. Math.: Sci. J. **11** (2022), no. 1, 1–15.

[39] S.G. Khavale and K.R. Gaikwad, *Two-dimensional generalized magneto-thermo-viscoelasticity problem for a spherical cavity with one relaxation time using fractional derivative*, Int. J. Thermodyn. **25** (2022), no. 2, 89–97.

[40] N. Noda, R.B. Hetnarski, Y. Tanigawa, *Thermal Stresses,* Second Edition, Taylor and Francis, New York, 2003.

[41] M.N. Ozisik, *Boundary Value Problem of Heat Conduction*, International Textbook Company, Scranton, Pennsylvania, pp. 84–101, 1968.